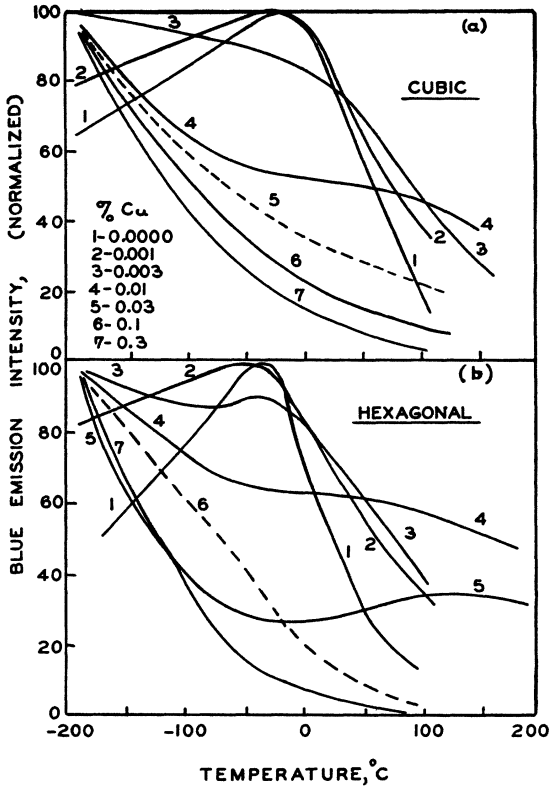

FIG. 2. Blue photo-luminescence emission intensity, as observed through a Wratten 47 filter, as a function of operating temperature, for a series of increasing copper proportions in cubic and hexagonal ZnS: [Zn]: Cu phosphors.

and between 0.03 and 0.1 percent copper for the hexagonal phosphors (1) a new blue band appears in the luminescence emission spectrum, (2) deep traps caused by the presence of copper in low proportions are destroyed, (3) some of the deeper traps present in the ZnS:[Zn] phosphor before the addition of any copper are destroyed, and (4) the temperature for maximum green intensity during excitation shifts to lower temperatures.

The close correlation between the shift of the temperature for maximum green intensity and the shift of the principal glow peaks for increasing copper proportions indicates that the efficiency maximum is due to an increase in the number of centers available for repetitive excitation as the traps are emptied by increasing the operating temperature. It has been shown[3,4] that an efficiency maximum is to be expected at temperatures corresponding to a large glow peak, if the number of excitable centers is limited and not very much larger than the number of traps.

* This letter is part of a dissertation presented to the faculty of the Physics Department of Princeton University in May, 1950, as partial fulfillment for the requirements of the Ph.D. degree.
† This work was done under contract between ONR and RCA.
[1] R. H. Bube, Phys. Rev. **80**, 655 (1950).
[2] R. H. Bube, Phys. Rev. **80**, 764 (1950).
[3] F. A. Kroeger, *Some Aspects of the Luminescence of Solids* (Elsevier Publishing Company, Inc., New York, 1948).
[4] R. H. Bube, J. Opt. Soc. Am. **39**, 681 (1949).

High Energy Photo-Protons from Carbon*

DARCY WALKER
Newman Laboratory of Nuclear Studies, Cornell University, Ithaca, New York
December 15, 1950

PROTONS with energies up to 124 Mev have been observed coming from a carbon target bombarded by γ-rays from an electron synchrotron operated at 195 Mev.

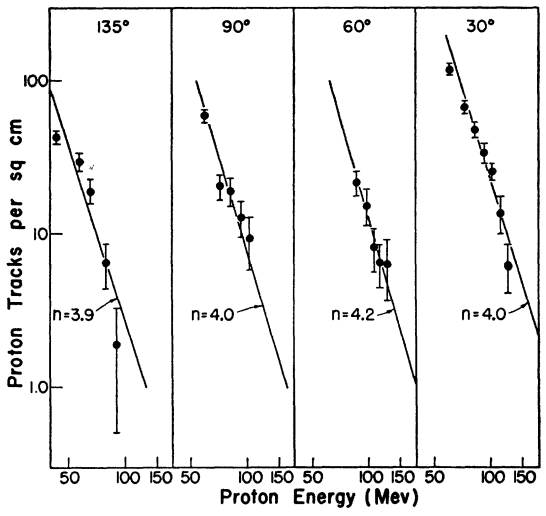

FIG. 1. Log-log plots of the density of proton tracks (N) in the emulsions of successive photographic plates against the proton energy (E) required for a proton to pass through each emulsion layer. Results are given for protons emitted at angles in the laboratory system of 135°, 90°, 60°, and 30° to the γ-ray beam. The track density is normalized to a target-emulsion distance of 22.8 cm. The errors shown are probable errors.

The γ-ray beam was passed through a 1.3-cm diameter hole in a lead block and allowed to impinge on a carbon plate 0.26 g/cm^2 thick placed at 45° to the beam. Disposed about the carbon target were four stacks of Ilford C-2 Nuclear Research plates interleaved with aluminum absorbers. These stacks recorded protons emitted from the target at angles of 135°, 90°, 60°, and 30° to the γ-ray beam, the over-all angular resolution being ±6°. The planes of the photographic plates were inclined at 30° to a line joining plate and target centers.

Figure 1 shows the form of the experimental results. The plots represent integral energy spectra. The lines give mean values of n, the spectra being represented by the form $N=N_0E^{-n}$. The value of n is about 4. This is a minimum value because the track counts corresponding to the lower energies tend to be too small, since (a) C-2 emulsions will not record protons with residual energies less than about 50 Mev and (b) blackening of the emulsion by

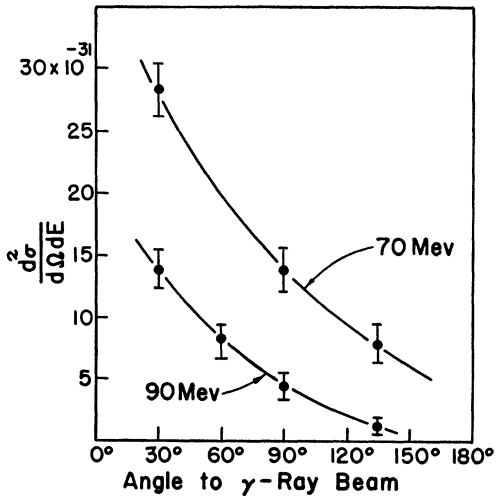

FIG. 2. Differential nuclear cross section of carbon for the production of protons plotted as a function of the angle of proton emission in the laboratory system. The differential nuclear cross section is expressed as square cm per steradian per Mev of proton energy (E) per unit Q. Results are shown for $E=70$ Mev and $E=90$ Mev.

electrons from the target becomes progressively more marked the nearer a plate to the target. The loss of counts due to (a) can be allowed for approximately; and if this is done, the value of n is increased from 4 to about 5. This value $n=5$ means that the number of protons per Mev of proton energy decreases as E^{-6}.

To derive absolute cross sections, a method due to Wilson[1] has been used. For the range of γ-ray energies in which we are interested, the average number of electrons produced by the cascade shower mechanism at a depth of 1 cm in lead is approximately $W/50$ for a γ-ray quantum of energy W Mev incident on the surface of the lead. The γ-ray beam, after passing through the target, impinged on a sheet of lead 1 cm thick, behind which was a flat aluminum ionization chamber 2.5 cm thick. If the number of quanta in the incident γ-ray spectrum between W and $W+dW$ is assumed to be QdW/W up to the maximum energy W_0, then the number of electrons traversing the ionization chamber is

$$\int_0^{W_0}(W/50)(Q/W)dW=QW_0/50.$$

These electrons traverse the ionization chamber at close to minimum ionization. Thus, the charge collected in the ionization chamber yields a value of Q, which is considered to be accurate to within a factor of 2.

Figure 2 shows the differential nuclear cross section plotted against the angle of emission of the protons for proton energies of 70 Mev and 90 Mev. These cross sections have been derived from the data of Fig. 1, allowance being made for protons not recorded owing to the limited sensitivity of C-2 emulsions. The probable errors shown relate to the relative values of the cross section at the various angles. The absolute values of the cross sections could be in error by as much as a factor of 3 when all sources of error are considered.

The strong forward bias in the angular distribution is inconsistent with a compound nucleus model. It agrees qualitatively with a two-nucleon model.[2] The strong decrease in cross section with increasing proton energy in the vicinity of 100 Mev, which is approximately half the maximum γ-ray energy, also lends support to a two-nucleon model.

The author would like to express his appreciation to Professor R. R. Wilson for the privilege of working in his laboratory and to the Commonwealth Fund for support.

* This work made use of facilities provided under a contract with the ONR.

[1] R. R. Wilson, private communication.
[2] J. Levinger, private communication.

The Nuclear Spin of Be^9

H. S. Gutowsky, R. E. McClure, and C. J. Hoffman
Noyes Chemical Laboratory, University of Illinois, Urbana, Illinois*
December 18, 1950

THE theoretically predicted and generally accepted value of 3/2 for the nuclear spin of Be^9 has had little experimental confirmation.[1] We have eliminated 1/2 as a possible value by observing the detailed line shape of the F^{19} magnetic resonance in vitreous BeF_2. Similar observations for K_2BeF_4 make a value of 5/2 unlikely. The nonappearance of hyperfine structure is further evidence[2] against this value. Thus, it appears that a value of 3/2 can now be assigned from experimental data.

The broadening of the F^{19} magnetic resonance in powdered beryllium compounds is predicted quantitatively by the second-moment equation[3]

$$\Delta H_2^2=(9/20)g_0^2\beta^2\Sigma_k r_{0k}^{-6}+(4/15)g_f^2\beta^2I_f(I_f+1)\Sigma_f r_{0f}^{-6}.$$

The subscripts 0, k, and f refer to a given fluorine nucleus, its fluorine, and its beryllium neighbors, respectively. In principle, I_f is obtained by the comparison of experimental second moments with the second moments computed from crystal structures and gyromagnetic ratios.

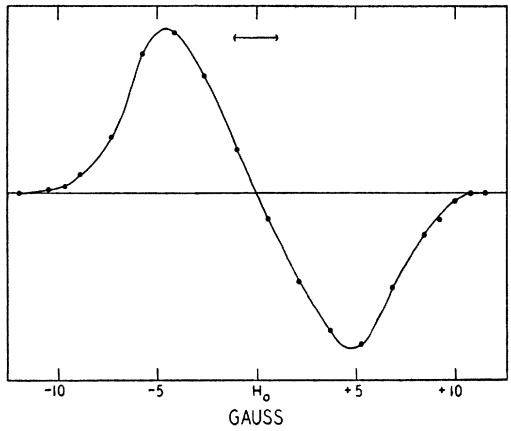

FIG. 1. The observed first derivative of the F^{19} magnetic resonance absorption line in vitreous BeF_2. The modulation is indicated by the horizontal arrow. The ordinate is in arbitrary units of intensity. H_0 is 6365 gauss.

The equipment and procedure used are similar to published accounts.[3,4] Vitreous BeF_2 was prepared by the thermal decomposition[5] of $(NH_4)_2BeF_4$. A typical derivative of the F^{19} magnetic resonance absorption line observed for this sample is given in Fig. 1. Four separate line plots gave second moments from 11.25 to 11.75 gauss^2, averaging 11.55 gauss^2, with a probable error of $\pm$0.15 gauss^2. No complete structural analysis appears to be available for BeF_2. The x-ray scattering curve for vitreous BeF_2 is compatible[5] with a random network structure and an assumed Be—F distance of 1.60A. However, Brandenberger[6] has made a determination of the unit cell size and symmetry of crystalline BeF_2 and suggests a Be—F distance of 1.53A. Lacking more detailed information, the spatial arrangement of Warren and Hill[5] was assumed; and theoretical second moments were computed as a function of the Be^9 spin and also the Be—F distance. These values are given in Table I. The Be—F distance of 1.46A required for agreement with a spin of 1/2 is impossibly small. The 1.53A distance[6] gives a spin of 3/2, while the 1.60A value[5] gives 5/2.

Observations were made on K_2BeF_4 to resolve the 3/2 *versus* 5/2 question. Three second moments were measured, ranging from 6.25 to 6.90 gauss^2, with an average of 6.65 gauss^2. In a partial analysis of the crystal structure[7] of $(NH_4)_2BeF_4$, tetrahedral $BeF_4^=$ groups were found, and a Be—F distance of 1.61A was suggested. When a Be^9 spin of 3/2 is used, the computed second moment for the $BeF_4^=$ group alone is 3.78 gauss^2. The broadening by nuclei outside the $BeF_4^=$ contributes an additional approximate[8] 2 gauss^2. Agreement between computed and experimental second moments can be achieved either by using a Be^9 spin of 5/2 or by decreasing the Be—F distance to about 1.57A. However, because of charge effects, the Be—F distance in the $BeF_4^=$ group should be slightly larger than in BeF_2. This criterion and the second-moment data can be satisfied most simply by assigning the spin of Be^9 as 3/2, and the Be—F distances as 1.57 and 1.52A in $BeF_4^=$ and BeF_2, respectively.

The desirability of further x-ray analysis of some of the beryllium fluorides is indicated by the above discussion. In addition, Rb_2BeF_4 is reported[8] to have the same crystal structure as K_2BeF_4 and $(NH_4)_2BeF_4$. The F^{19} magnetic resonance lines in the latter compounds are simple, being quite similar in shape to that in BeF_2 indicated by the derivative in Fig. 1. However, the F^{19} resonance

TABLE I. The second moment of the F^{19} magnetic resonance in vitreous BeF_2 as a function of Be^9 spin and Be-F distance.

r of Be-F		1.60A	1.515A	1.46A
I of Be^9	1/2	6.75 gauss^2	9.40 gauss^2	11.55 gauss^2
	3/2	8.30	11.55	14.20
	5/2	10.85	15.15	18.55